Supplementary Information

Engineering Multiwalled Carbon Nanotubes Modified Titanium Carbide MXene Nanocomposites for Flexible Symmetric Supercapacitors in Printed Electronics

S.M. Varghese [a,b], A.S. Pillai [c,b], Surendran Kuzhichalil Peethambharan [c,b*], R.B. Rakhi [a,b*]

[a] Centre for Sustainable Energy Technologies (C-SET), CSIR-National Institute for Interdisciplinary Science and Technology, Industrial Estate, Thiruvananthapuram - 695 019, Kerala, India

[b] Academy of Scientific and Innovative Research (AcSIR), Ghaziabad- 201002, India.

[c] Materials Science and Technology Division, CSIR-National Institute for Interdisciplinary Science and Technology, Industrial Estate, Thiruvananthapuram - 695 019, Kerala, India.

* Corresponding author: Tel.: +91-471-2515474, +91-471-2515411. Fax: +91-471-2491712.

E-mail: rakhiraghavanbaby@niist.res.in, kpsurendran@niist.res.in

1. Experimental Details

1.1 Chemicals

Titanium aluminium carbide (Ti_3AlC_2, MAX phase 312, ≥90%, ≤40 μm particle size), lithium fluoride (LiF, ≥99.99% trace metal basis), hydrochloric acid (HCl, 37%, analytical grade), and dimethyl sulfoxide (DMSO), multi-walled carbon nanotubes (MWCNTs), PEDOT:PSS pellets (sheet resistance: 200–450 Ω/□), ethylene glycol (EG, anhydrous, 99.8%), sodium dodecyl sulfate (SDS), dimethylformamide (DMF), ethanol (anhydrous, 99%), potassium hydroxide (KOH) pellets, lithium perchlorate ($LiClO_4$), polytetrafluoroethylene (PTFE), poly(methyl methacrylate) (PMMA), fumed silica (FS), and propylene carbonate (PC). Additionally, conductive silver ink was procured from Metalon 03LV, *NovaCentrix*, Austin, USA.

1.2 Synthesis of MXene and delaminated MXene

The two-dimensional titanium carbide ($Ti_3C_2T_x$) MXene nanosheets were synthesized from Ti_3AlC_2 (MAX phase) using a procedure similar to the one outlined in our previous work[1]. To selectively etch the MAX phase, a specific amount of Ti_3AlC_2 (2 g) was immersed in a mixture of 9 M HCl (40 ml) and LiF (3.2 g) and maintained at 35 ± 1 ºC for 24 hours. The resulting suspension was ultrasonicated in water for 1 hour under an argon (Ar) atmosphere to exfoliate multilayered MXene into few-layer nanosheets, followed by filtration and vacuum drying at 70 °C for 12 hours. The prepared MXenes were annealed at 200 °C for 2 hours in N_2 atmosphere to stabilize the sample [2]. The sample underwent delamination using DMSO as the intercalant. MXene was stirred with DMSO (1 g:20 mL) for 1 hours at room temperature, followed by centrifugation to separate the intercalated powder. After decanting the supernatant, deionized water (1 g:500 mL) was added to the residue, and the mixture was ultrasonicated for 2 hours. The resulting suspension was centrifuged, and the supernatant was filtered through a PTFE membrane (47 mm diameter, 0.2 μm pore size). Finally, the filtered sample was dried in

an oven at 60 °C for 24 hours, obtaining delaminated MXene (D-MXene)[3]. The schematic diagram for the synthesis of MXene and D-MXene is depicted in **Figure 1**

1.3 Fabrication and electrochemical performance study of D-MXene/MWCNT composite electrodes

The delaminated MXene was further used for the preparation of D-MXene/MWCNT composites. The different compositions of the synthesized D-MXene and multi-walled carbon nanotubes (MWCNTs) composites were prepared using a straightforward sonication process. Initially, 5 wt.% of MWCNTs in anhydrous ethanol were added to a 95 wt.% MXene solution to prepare the D-MXene/MWCNT dispersion. The mixture was then mechanically stirred with a magnetic stirrer for 1 hour to ensure thorough mixing. Subsequently, it was ultrasonicated at room temperature for 3 hours to achieve a stable and homogeneous dispersion. Following this procedure, D-MXene/MWCNT composites with different MWCNTs weight percentages (10%, 20%, 30%, and 40%) were prepared. These composites were denoted as MC-10, MC-20, MC-30, and MC-40, respectively, with the initial 5 wt.% composition referred to as MC-5. The required amount of these composites along with PTFE binder and acetylene black in a weight ratio 8:1:1 was used as electrodes for the fabrication of supercapacitors. The electrode slurry was drop-cast onto square patches (1 cm^2) of conductive carbon cloth substrate and subsequently dried in an oven at 60 °C overnight to ensure complete solvent evaporation and firm adhesion of the composite material. The carbon cloth substrates were weighed before and after coating, yielding an active material mass loading of approximately 1 mg/cm^2 per electrode. Symmetric supercapacitors were fabricated by vertically stacking the fabricated electrodes face-to-face with a Celgard 3501 separator sandwiched between them. The separator was soaked in the liquid electrolyte (6 M KOH) before assembling. The electrochemical properties of the fabricated supercapacitors were subsequently evaluated using a two-electrode configuration after an infiltration period of 24 hours.

1.4 Formulation and printing of the D-MXene/MWCNT/PEDOT: PSS (MCP) ink

To prepare the MCP ink, the conducting polymer PEDOT: PSS was used as a binder, and SDS was used as the dispersant. Delaminated MXene, PEDOT: PSS, and multi-walled CNTs dispersions were independently prepared through a sonication process with temperature control and intermediate stirring. Dispersions of D-MXene were prepared by introducing 168 mg of the wet precipitate into a 1:1 mixture of ethanol and DMF. The mixture was then sonicated for 12 hours with intermediate stirring (magnetic stirring, 1500 rpm) for 15 minutes after every hour. Similarly, MWCNTs were dispersed by introducing 42 mg into 1 mL ethanol containing 4 mg SDS. 21 mg (8.9 wt% of total solid loading) PEDOT: PSS was dispersed in 2 mL mixture of 0.7:0.3 ethanol and ethylene glycol, respectively. The ink was then prepared by mixing the dispersions in the volume ratio 0.5:1:1.4 (D-MXene/MWCNT/PEDOT: PSS), such that the optimized ratio of D-MXene/MWCNT for better electrode characteristics is maintained. The ternary mixture was then sonicated for 12 hours at 40 ºC and mixed using magnetic stirring for 24 hours to obtain a stable ink. The prepared ink was refrigerated until printing.

Prior to printing, the electrochemical performance was evaluated by uniformly coating the optimally formulated ink (~0.5 mg cm^{-2}) onto a 1 cm^2 conductive carbon cloth and drying it at 100 °C. The symmetric supercapacitors were assembled by stacking the electrodes in a face-to-face fashion, separated by a Celgard 3501 membrane, pre-dipped in a 6 M KOH electrolyte. The assembled device was kept overnight before performance testing. The optimized ink was then used to print rectangular test patterns on a Mylar® substrate through a 25-mesh screen using a semi-automatic screen and stencil printer (XPRT2, Ekra, Bönnigheim, Germany). Each pattern was printed through a four-stroke print cycle, with a print pressure of 1.2 bar and a forward print speed of 25 mm/s. The printed patterns were then cured at 100 ºC in a hot air oven for 30 minutes and stored under ambient conditions.

1.5 Formulation of gel-polymer electrolyte

The selection of suitable electrolytes is a crucial aspect of developing printed micro-supercapacitors. As the main focus is to introduce a flexible real-time supercapacitor, that is resistant to leakage issues, we have chosen, polymer-based gel electrolytes for the fabrication of supercapacitors. Gel polymer electrolyte comprises of a polymer matrix with ionic conductors dispersed in a plasticizer. The crystalline matrix of the polymer forms the gel's skeleton while the liquid phase facilitates the ion transport. To improve the conductivity and mechanical properties, fillers are often incorporated. Here, a gel-polymer electrolyte (GPE) for developing micro-supercapacitors was formulated using $LiClO_4$ as the active material dispersed in a matrix of PMMA, using PC as the plasticizer and fumed silica as the filler. To prepare the GPE, 1 M $LiClO_4$ solution was initially prepared in 3.97 mL PC, followed by adding 20 mg of FS in four equal parts (part of 5 mg each). After complete addition, the mixture was mechanically stirred for 4 hours using a magnetic stirrer at 1300 rpm. 0.5 g of PMMA was added to the mixture, stirred for 2 hours, and then transferred into an oil bath at 90 ºC. After heating for nearly 24 hours, the mixture was slowly quenched to room temperature to obtain the transparent, thick GPE. The prepared GPE was de-aired in a vacuum chamber for 2 hours and refrigerated until further use.

1.6 Fabrication of printed micro-supercapacitors (MSCs)

All printed MSCs were fabricated through a multistep printing process. Each MSC employed a planar interdigital electrode (IDE) geometry consisting of three pairs of interdigitated fingers, where each finger had a length of 1 cm, width of 1 mm, and an inter-finger gap of 500 µm, defining the effective active area of the device. The electrode thickness, measured by surface profilometry, was approximately 23.31 ± 0.14 µm, while the effective active electrode area defined by the interdigital region was ~0.5 cm^2. The total active electrode mass deposited within this area was approximately 0.7 mg, corresponding to an areal mass density of ~1.5 mg cm^{-2}.

Prior to the printing of the IDEs, IDE-type bottom current collectors (bottom CC) were first printed onto Mylar® substrate using conductive silver ink. This process was carried out with a semiautomatic screen printer through a 325-mesh screen (two strokes, print speed - 40 mm/s). After drying for 3 hours at 100 ℃, it was then carefully aligned with another screen to print the IDE, employing the printer's manual optical positioning system. IDEs were then printed using the MCP ink, using a 25-mesh screen, and dried at 100 ºC for 30 minutes. The dried electrodes were then carefully aligned to print the top current collectors (top CC) using conductive silver ink (Metalon 03LV, *NovaCentrix*, Austin, USA) through a 325-mesh screen. After curing at 100 ℃ for 3 hours, the prepared GPE was printed using doctor blading on the IDE through laser cut stencils of thickness 80 µm. The entire structure was de-aired in a vacuum chamber for 2 hours to achieve the fully printed MSC. The MSC was encapsulated using vacuum sealing and edge lamination using PET sheets. Before the encapsulation, a hollow PDMS spacer with a thickness of 2 mm was attached to the IDE, which prevented the spreading of GPE. A detailed representation of this multi-step printing process is depicted in **Figure 1**. The electrochemical evaluation of MSCs was evaluated after an infiltration period of 24 hours.

1.7 Material characterization

The electrode materials were extensively characterized through various techniques, including Powder X-ray diffraction (PXRD) and Wide-angle X-ray diffraction (WXRD) , Brunauer-Emmett-Teller (BET) surface analysis, scanning electron microscopy (SEM), and transmission electron microscopy (TEM). An automated XRD system (Bruker D8 Advance (40 kV, 40 mA) with Cu Kα radiation (λ = 1.54 Å) and XEUSS SAXS/WAXS system equipped with Cu Kα radiation (λ = 1.54 Å) (Xenocs operating at 50 kV and 0.6 mA) was used to study the crystallographic structure and phase purity of the samples. SEM (ZEISS EVO 18 Special Edition) was employed to investigate the microstructure and surface morphology, while TEM

was conducted on a Tecnai G230 LaB6 microscope for detailed morphological examination. The BET surface area, pore size distribution and pore diameter were measured using a Nova Touch LX4 analyzer, providing valuable insights into the material's porous architecture.

1.8 Characterization of ink and printed structures

Various characterization techniques were employed to thoroughly evaluate the inks, printed patterns, and fabricated supercapacitors. The electrical properties of the printed structures were examined using the four-probe method, utilizing a Keithley 2450 source meter. The surface morphology of the printed films was analyzed through SEM (Zeiss EVO 50) and optical imaging (Leica – DMRX). The surface tension of the fabricated ink was measured at 22.6 ºC using a pendant drop test with a tensiometer, while the contact angle with Mylar® was determined using a sessile drop test (DSA 30, KRÜSS GmbH, Hamburg, Germany). The flow properties of the inks were investigated using a rheometer (Rheoplus, Anton Paar, Graz, Austria).

1.9 Electrochemical measurements

The electrochemical performance studies of the fabricated composite electrodes and printed IDEs were evaluated using the techniques, including CV, GCD and EIS using a VMP-3 Biologic, France in a two-electrode configuration with an automatic 80% IR compensation enabled. CV measurements were conducted within a voltage range of 0-0.8 V in both KOH and gel polymer electrolytes, using scan rates between 5 mV s^{-1} and 200 mV s^{-1}. GCD profiles were carried out at various charge-discharge rates within the operating potential range of 0-0.8 V. EIS measurements were performed across a frequency range of 10 mHz to 100 kHz at open-circuit voltage, applying a 5-mV amplitude. An electronic balance (Shimadzu Corporation) was used to measure the weight of the electrodes printed on Mylar® and conductive carbon paper

before and after deposition. Bending studies of micro-supercapacitors (MSCs) were conducted using a custom setup, with bending-cycle testing performed at 4 Hz on a modified triboelectric measurement system (Holmarc, India).

2. Calculations

2.1. D-MXene/MWCNT based supercapacitor electrodes

The electrochemical properties of the supercapacitor electrodes were examined using symmetric assemblies of each material in a two-electrode configuration, employing cyclic voltammetry (CV), galvanostatic charge-discharge (GCD), and electrochemical impedance spectroscopy (EIS).

The specific capacitance (C_{sp}) of D-MXene and their composites was calculated using the following equations:

$$From\ CV,\ C_{sp} = \frac{2}{m\,\Delta V\,s}\int i(V)dV \qquad \text{(S1)}$$

$$From\ GCD,\ C_{sp} = \frac{2i}{m(\Delta V/\Delta t)} \qquad \text{(S2)}$$

Where, "C_{sp}" denotes the specific capacitance, $\int i(V)dV$ is the integrated area under the current-voltage curve, "i" the constant current for charge-discharge (mA), "$^{\Delta V}/_{\Delta t}$" is the slope of the discharge curve and "m", active mass on a single electrode. The mass loading of the active material on the electrodes was about 1 mg/cm^2.

The energy density (E_D) and power density (P_D) of the electrodes were calculated using the following equations:

$$E_D = \frac{C_{sp} \times V^2}{2 \times 3.6} \quad (Wh\,kg^{-1}) \qquad (S3)$$

$$P_D = \frac{E_{sp}}{\Delta t} \times 3600 \quad (W\,kg^{-1}) \qquad (S4)$$

“V” represents operating potential window, Δt is the discharge time obtained from the galvanostatic charge-discharge (GCD) profiles, E_D refers the energy density and P_D represents the power density.

For practical assessment at the device level, the energy density of the symmetric two-electrode cell was calculated by accounting for the total active mass of both electrodes. This results in a fourfold reduction compared to single-electrode values. The device-level gravimetric energy density was calculated as:

$E_{cell} = \frac{1}{2} C_{sp,cell} V_{cell}^{2}$ $(S5)$where V_{cell} is the operating voltage window and the device-level specific capacitance is given by

$$C_{sp,cell} = \frac{1}{4} C_{sp,electrode} \qquad (S6)$$

2.2. D-MXene/MWCNT/PEDOT:PSS based printed electrodes

To calculate areal capacitance (C_{areal}), of the D-MXene/MWCNT/PEDOT:PSS based printed electrodes, the following equations were used

$$C_{areal} = \frac{2}{a\,\Delta V\,s} \int i(V)dV \qquad \text{(S7)}$$

$$C_{areal} = \frac{2i}{a(\Delta V/\Delta t)} \qquad \text{(S8)}$$

Here,"C_{areal}" denotes the areal capacitance, $\int i(V)dV$ is the integrated area under the current-voltage curve ,“i” denotes the constant current for charge-discharge (mA), "s" is the potential scan rate, "$\Delta V/\Delta t$" is the slope of the discharge curve and "a", the active area of the interdigitated electrode. The active electrode area was about 0.5 cm^2 with an areal mass density of 1.5 mg/cm^2.

The volumetric capacitance (C_{vol} in F cm^{-3}) of the device was calculated using the relation:

$$C_{vol} = \frac{2i}{a \times t \times \left(\frac{\Delta V}{\Delta t}\right)}$$

where "t" is the thickness of the electrode (cm). The thickness of the printed electrode is about 23.3 µm.

The areal energy density (E_{Areal}) and areal power density (P_{Areal}) of MSC were calculated using the following equations:

$$E_{Areal} = \frac{C_{Areal} \times V^2}{2} \qquad (S9)$$

$$P_{Areal} = \frac{E_{Areal}}{\Delta t} \qquad (S10)$$

"V" represents operating potential window, Δt is the discharge time obtained from the galvanostatic charge–discharge (GCD) profiles, E_{Areal} refers the areal energy density and P_{Areal} represents the areal power density.

Similarly, the volumetric energy density (E_{Vol}) and volumetric power density (P_{Vol}) of MSC were calculated using the following equations:

$$E_{Vol} = \frac{C_{Vol} \times V^2}{2} \qquad (S11)$$

$$P_{Vol} = \frac{E_{Vol}}{\Delta t} \qquad (S12)$$

3. Supplementary figures

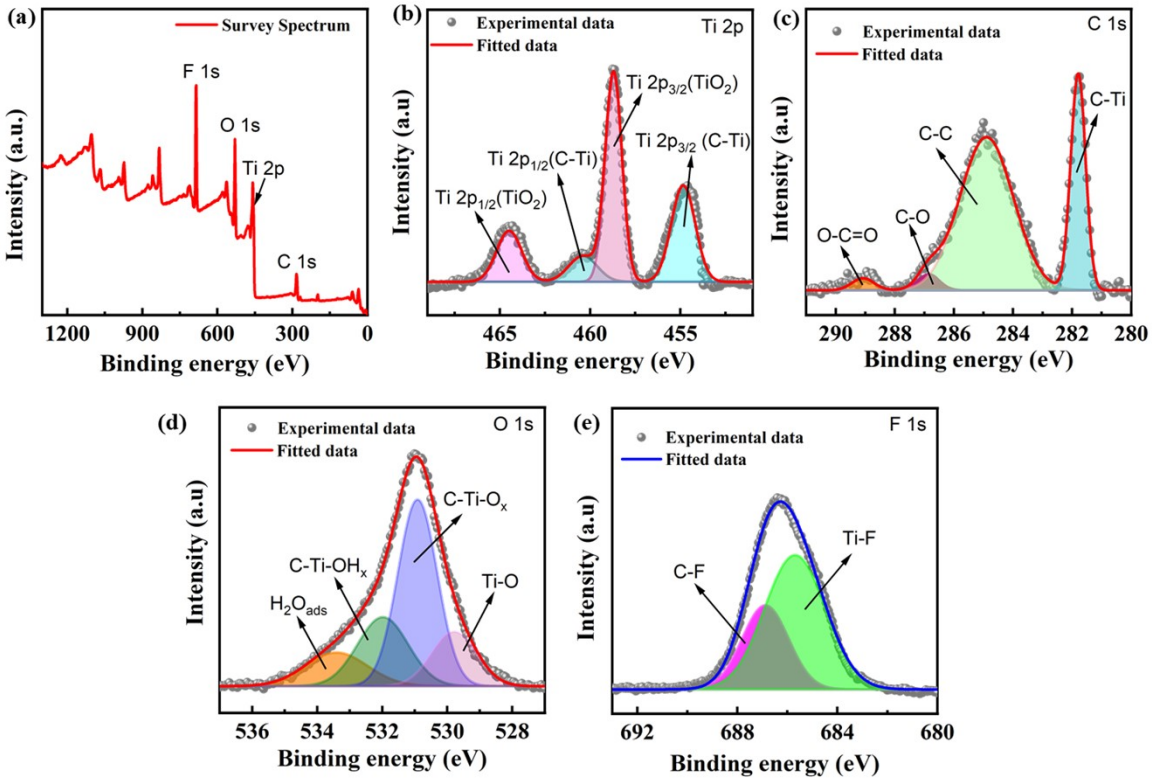

Figure S1: (a) Survey spectra and Deconvoluted XPS spectra of (b) Ti 2p, (c) C 1s (d) O 1s (e) F 1s of D-MXene.

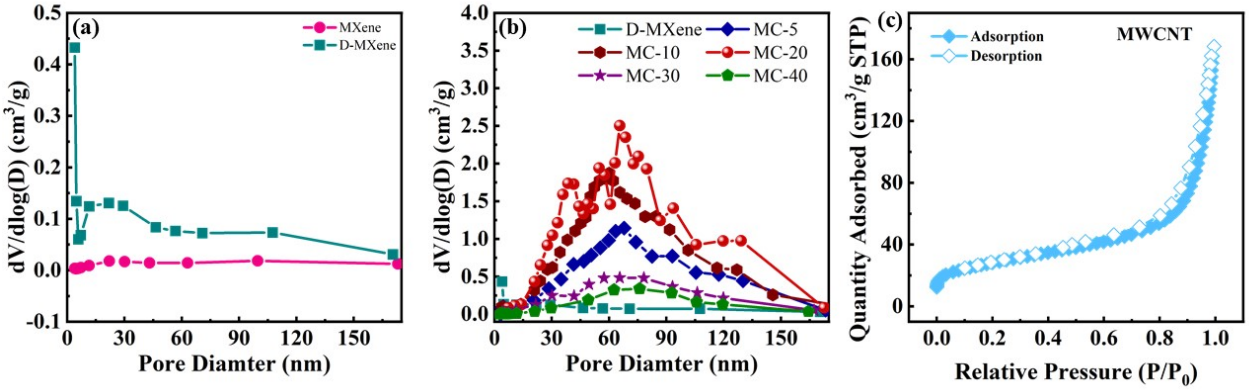

Figure S2: *The pore size distribution of (a) $Ti_3C_2T_x$ MXene and D-MXene (b) D-MXene/MWCNT composites (c) BET isotherm of MWCNT.*

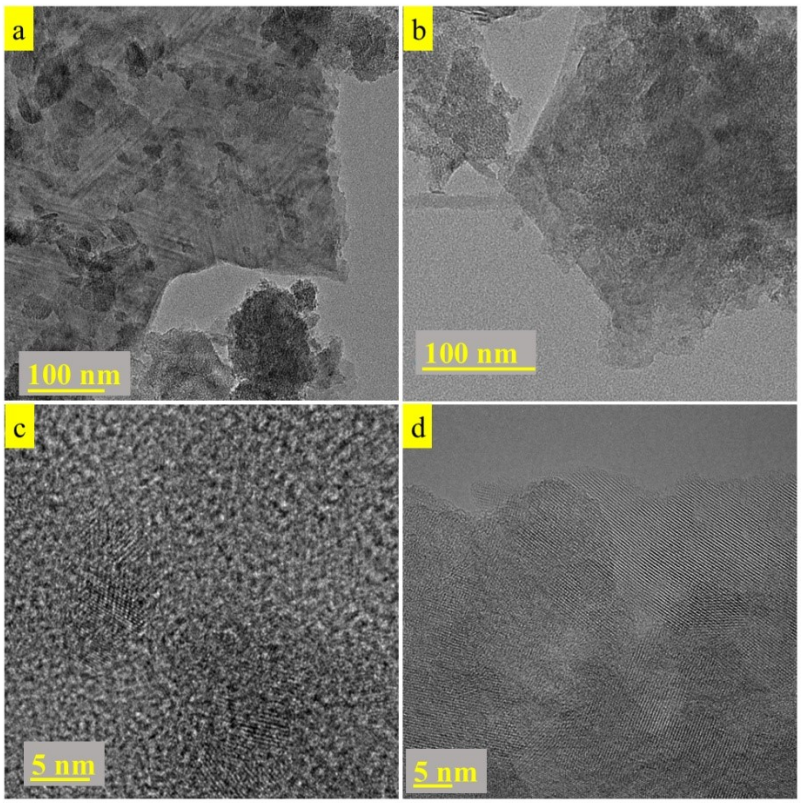

Figure S3: (a,b) low-magnification and (c,d) high-magnification TEM images of MXene and D-MXene

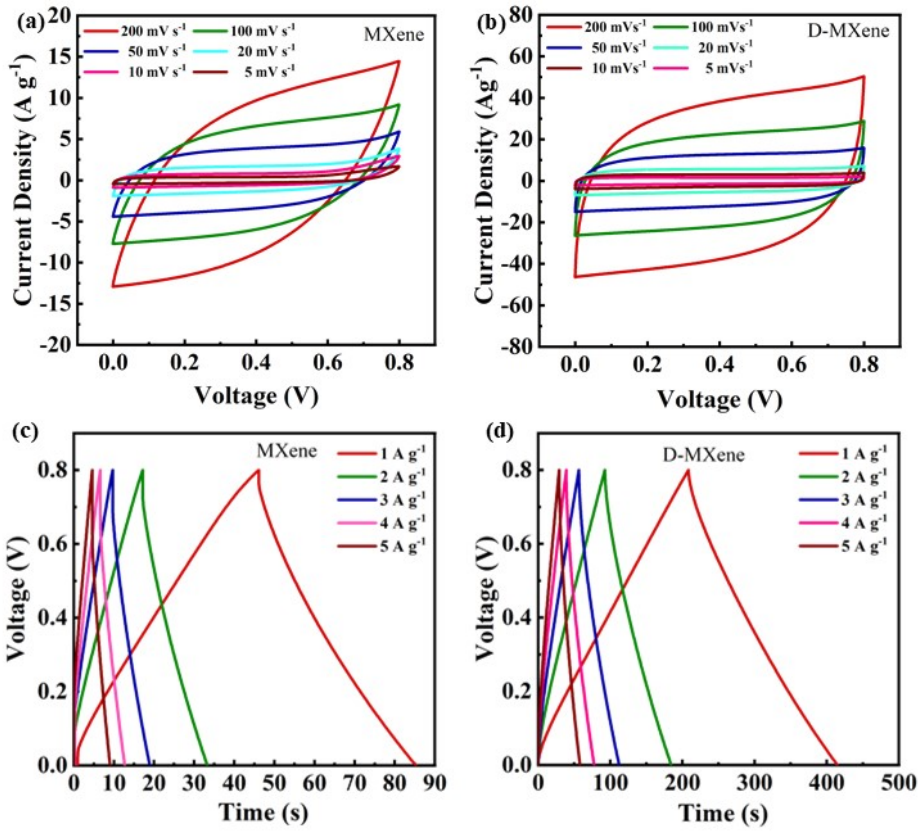

Figure S4: Electrochemical performance studies of the fabricated MXene, and D-MXene electrodes: *(a,b) Cyclic Voltammograms from 5 mV s^{-1} to 200 mVs^{-1}*, *(c,d) GCD curves at 1 A g^{-1} to 5 Ag^{-1}*.

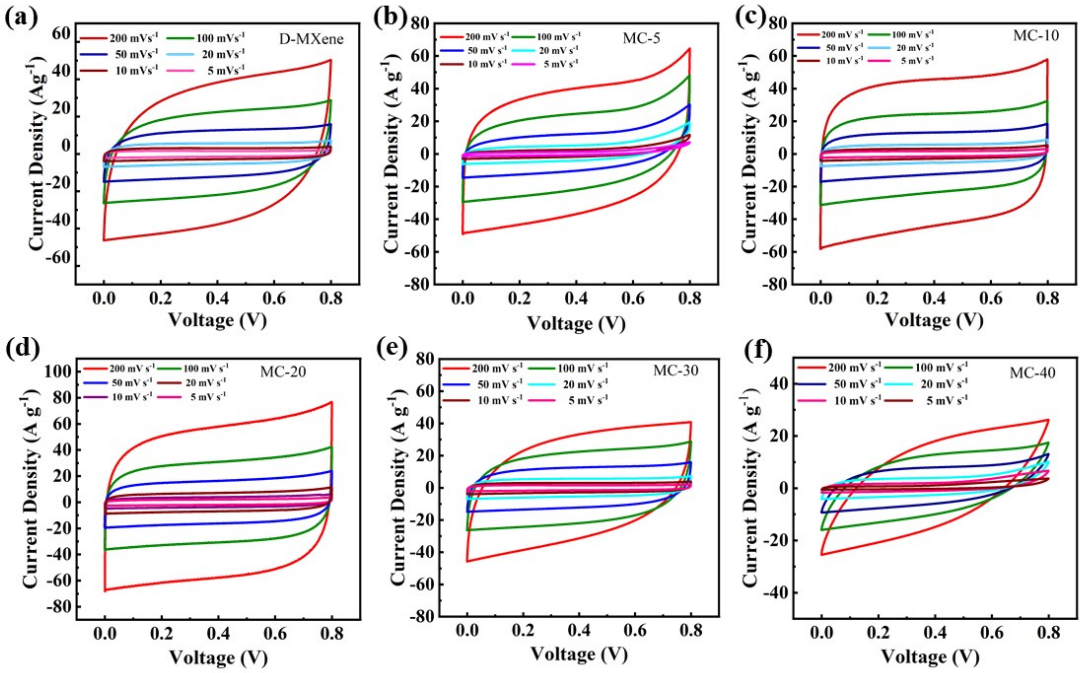

Figure S5: Electrochemical characteristics of the fabricated D-MXene, and D-MXene/MWCNT composite electrodes *(a-f) Cyclic voltammograms at scan rates ranging from 5 mV s^{-1} to 200 mV s^{-1}.*

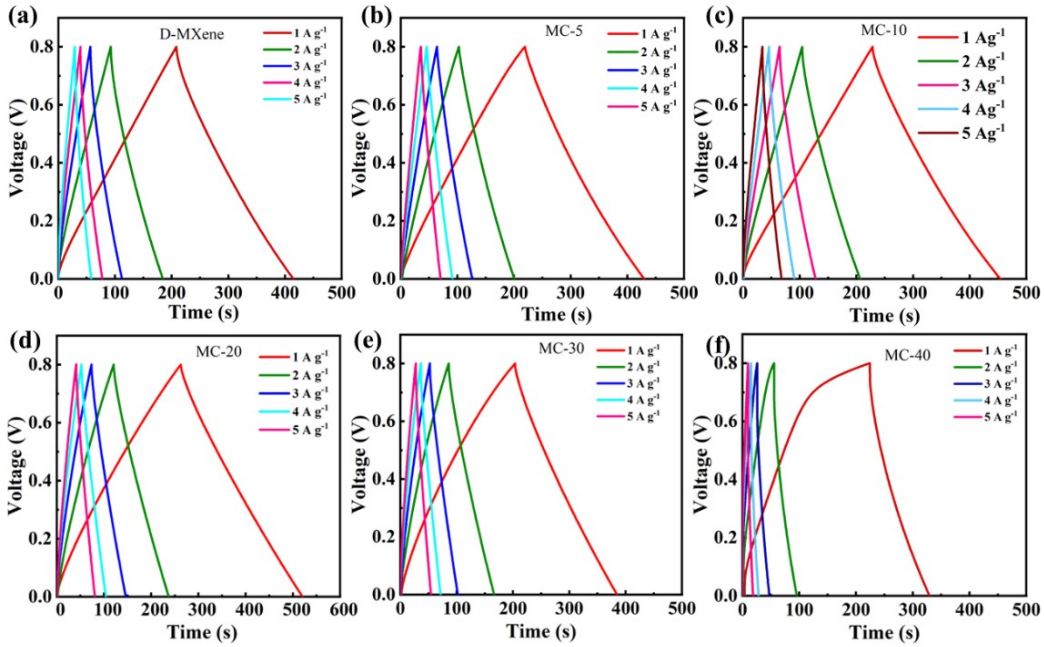

Figure S6:*(a-f) Galvanostatic Charge Discharge curves of D-MXene/MWCNT composites at current densities ranging from 1 A g^{-1} to 5 A g^{-1}.*

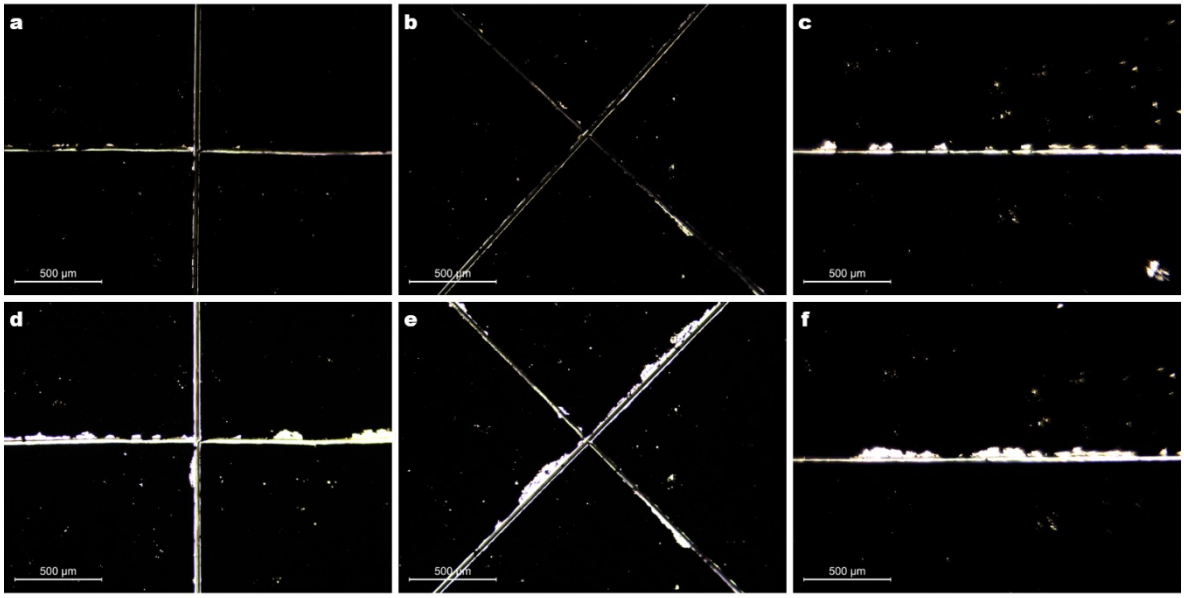

Figure S7: Adhesion test of MCP ink printed on Mylar dried at 100 °C for thirty minutes. *(a), (c), and (e) optical micrographs of the printed surface before peeling off. (b), (d), and (f) optical micrographs of the printed surface after peel-off*

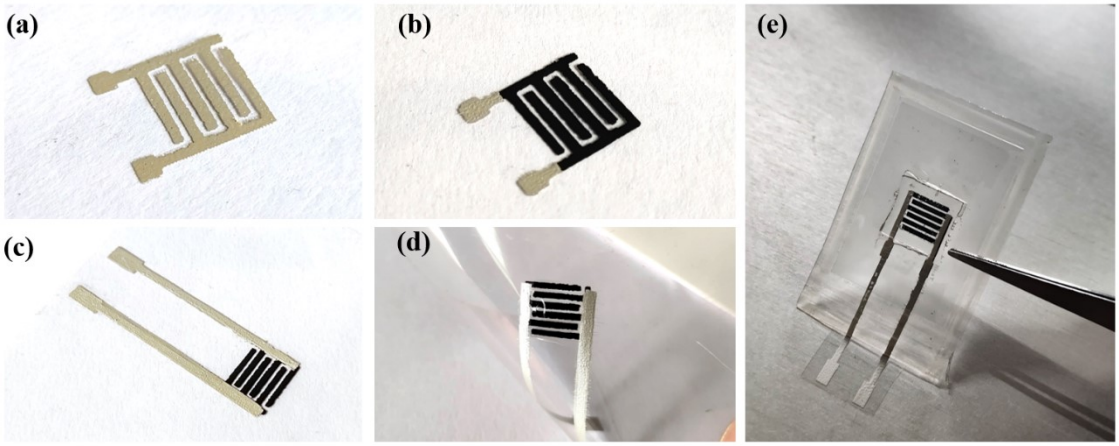

Figure S8: Photographs during the MSC fabrication process. *After printing (a) bottom CC, (b) IDE, (c) top CC, (d) GPE, and (e) encapsulation*

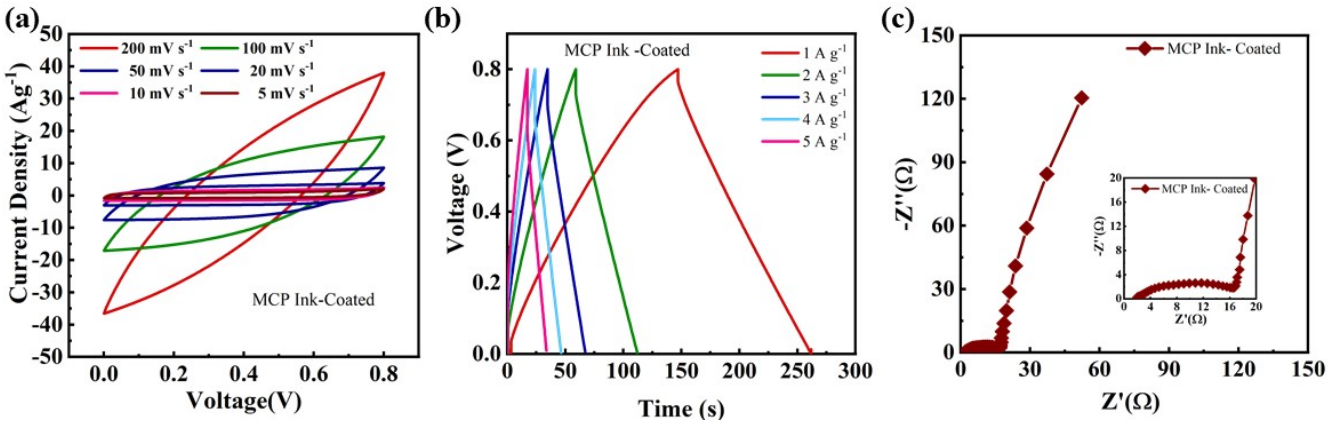

Figure S9: Electrochemical characteristics of D-MXene/MWCNT/PEDOT:PSS (MCP) ink coated on carbon cloth. *(a)CV studies conducted at scan rates ranging from 5 mV s^{-1} to 200 mV s^{-1}, (b) GCD curves at current densities ranging from 1 A g^{-1} to 5 A g^{-1}, and (c) Nyquist plot.*

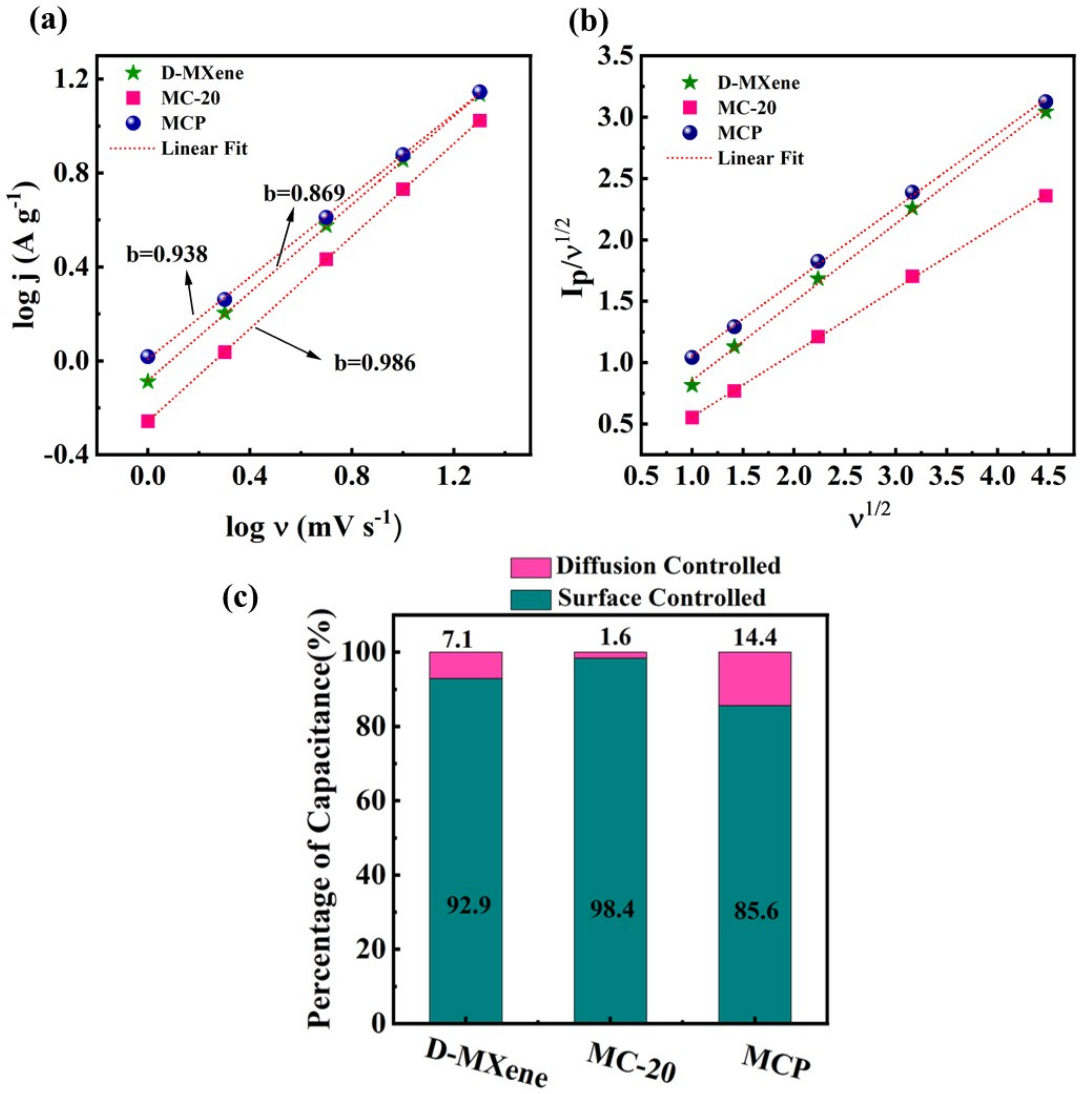

Figure S10: Linear fitting of (A) log(j) vs log(ν), (B) Ip/$\sqrt{\nu}$ vs $\sqrt{\nu}$, and (C) surface-controlled and diffusion-controlled charge-storage contributions of D-MXene, MC-20, and MCP electrodes, calculated using Dunn's method.

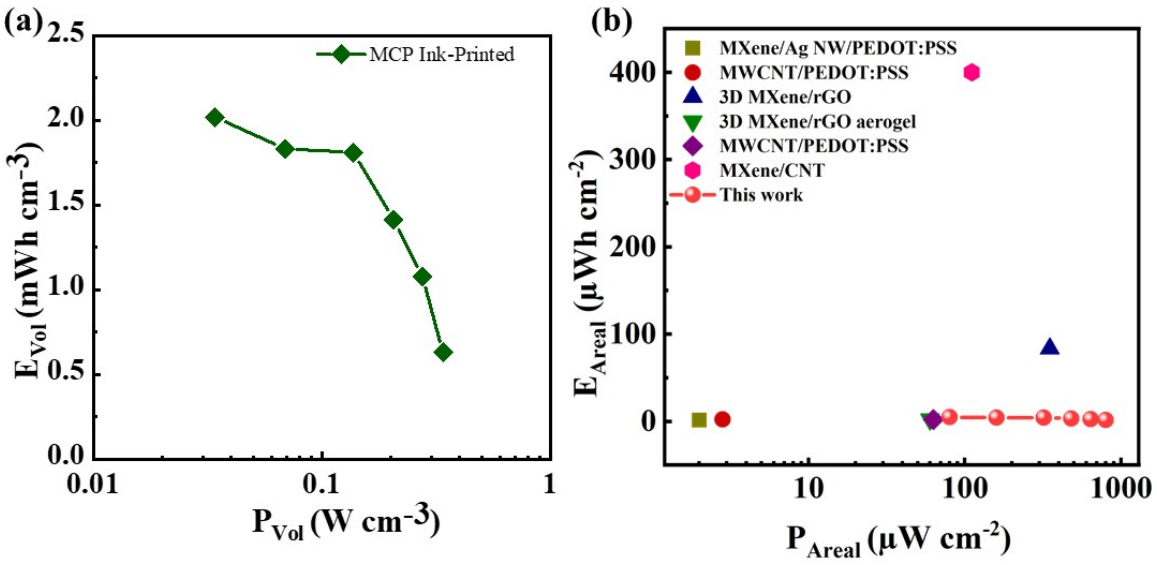

Figure S11: Ragone plot (a) showing volumetric energy and power densities of the printed MSC, (b) comparing the area energy and power density of our work with previously reported MSCs

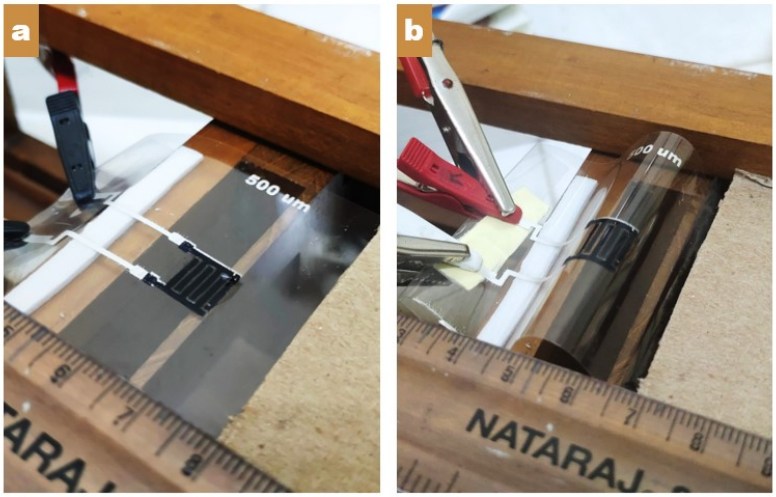

Figure S12. *Photographs of the fabricated MSC under bending test when bending diameter is (a) zero, (b) 1.0 cm.*

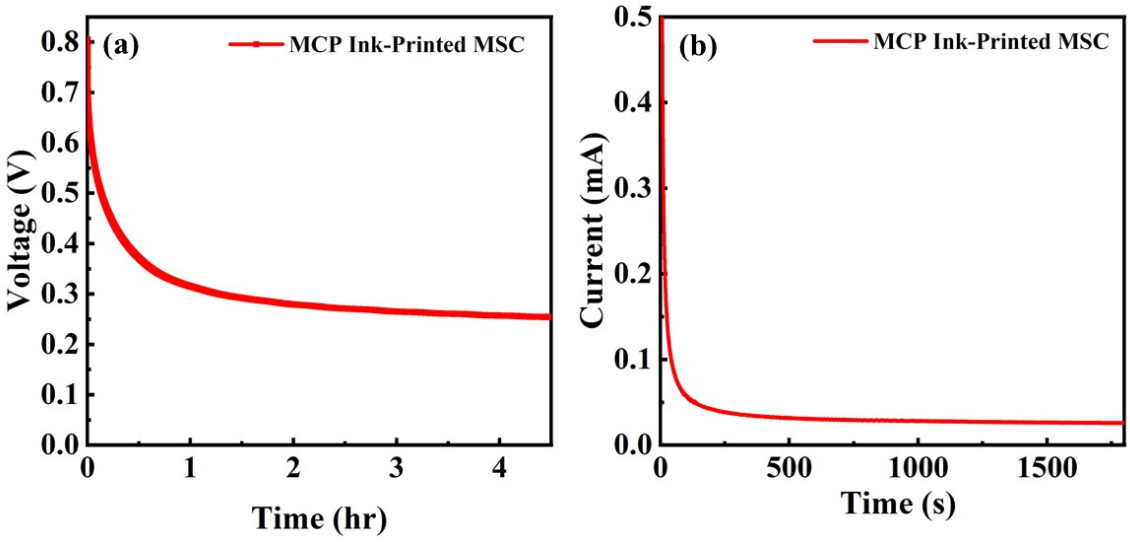

Figure S13: (a) Leakage current, and (b) Self-discharge profiles of the printed MSC

4. Supporting Tables

Table S1: . *BET surface area, BJH desorption average pore diameter and BJH desorption cumulative pore volume values of all samples obtained from nitrogen adsorption-desorption isotherms.*

Electrode Material	BET surface area (m^2/g)	BJH desorption average pore diameter (nm)	BJH desorption Cumulative Pore Volume (cm^3/g)
MXene	4.45	24.71	0.027
D-MXene	43.63	10.99	0.178
MC-5	70.66	30.05	0.595
MC-10	105.05	33.21	0.939
MC-20	112.04	37.87	1.162
MC-30	35.71	28.85	0.3147
MC-40	16.25	38.54	0.172

Table S2*: The specific capacitance values of of $Ti_3C_2T_x$ MXene, D-MXene and D-MXene/MWCNT composites calculated from CV.*

Scan rate [mV s^{-1}]	Specific capacitance [F g^{-1}]						
	MXene	**D-MXene**	**MC-5**	**MC-10**	**MC-20**	**MC-30**	**MC-40**
200	87	358	369	436	556	292	158
100	115	405	447	472	594	406	211
50	135	461	463	522	633	462	269
20	155	525	554	561	699	527	381
10	168	575	578	601	755	579	402
5	178	603	615	635	801	604	410

Table S3*: The specific capacitance values of MXene, D-MXene and D-MXene/MWCNT composites calculated from GCD.*

Current Dens [A g^{-1}]	Specific capacitance [F g^{-1}]						
	MXene	D-MXene	MC-5	MC-10	MC-20	MC-30	MC-40
1	98	516	526	564	645	457	262
2	82	462	489	517	592	403	201
3	69	425	463	475	550	380	161
4	62	387	452	456	518	352	133
5	60	361	441	449	497	341	117

Table S4: The electrochemical performance evaluation for all the samples: *The solution resistance, charge transfer resistance, energy density, power density and the cyclic stability data.*

Electrode Material	R_s [ohm]	R_{ct} [ohm]	Energy Density [Wh kg^{-1}]	Power Density [W kg^{-1}]	Cyclic Stability [%]
MXene	1.42	5.81	8.71	798.9	90
D-MXene	1.21	4.13	45.87	800.1	92
MC-5	1.24	1.21	46.76	800.3	86
MC-10	1.22	1.34	50.13	801.1	86
MC-20	1.22	1.17	57.34	802.7	88
MC-30	1.34	1.47	40.62	799.1	85
MC-40	1.37	2.82	23.29	798.8	84

Table S5: Energy density and power density values calculated at the single-electrode and device level for MXene and D-MXene electrodes.

MXene				D-MXene			
E_D (single) Wh kg^{-1}	E_D(cell) Wh kg^{-1}	P_D(single) W kg^{-1}	P_D (cell) W kg^{-1}	E_D (single) Wh kg^{-1}	E_D (cell) Wh kg^{-1}	P_D (single) W kg^{-1}	P_D (cell) W kg^{-1}

8.71	2.18	798.9	199.7	45.9	11.47	800.1	200.03
7.29	1.82	1340	335	41.07	10.26	1601.5	400.36
6.13	1.53	2381	595.25	37.78	9.44	2405.6	601.4
5.51	1.38	3221	805.25	34.4	8.60	3206.7	801.68
5.33	1.33	4024	1006	32.09	8.02	4022	1005.5

Table S6: Energy density values calculated at the single-electrode and device level for D-MXene/MWCNT composites

MC-5		**MC-10**		**MC-20**		**MC-30**		**MC-40**	
E_D (single) Wh kg^{-1}	**E_D (cell) Wh kg^{-1}**	**E_D (single) Wh kg^{-1}**	**E_D (cell) Wh kg^{-1}**	**E_D (single) Wh kg^{-1}**	**E_D (cell) Wh kg^{-1}**	**E_D (single) Wh kg^{-1}**	**E_D (cell) Wh kg^{-1}**	**E_D (single) Wh kg^{-1}**	**E_D (cell) Wh kg^{-1}**
46.76	11.69	50.13	12.53	57.34	14.33	40.62	10.15	23.29	5.82
43.47	10.87	45.96	11.49	52.63	13.16	35.62	8.905	17.86	4.46
41.16	10.29	42.22	10.55	48.89	12.22	33.78	8.445	14.31	3.58
40.18	10.04	40.53	10.13	46.05	11.51	31.29	7.82	11.82	2.95
39.20	9.80	39.91	9.98	44.18	11.04	30.31	7.58	10.40	2.60

Table S7: Power density values calculated at the single-electrode and device level for D-MXene/MWCNT composites

MC-5		**MC-10**		**MC-20**		**MC-30**		**MC-40**	
P_D (single) W kg^{-1}	**P_D (cell) W kg^{-1}**	**P_D (single) W kg^{-1}**	**P_D (cell) W kg^{-1}**	**P_D (single) W kg^{-1}**	**P_D (cell) W kg^{-1}**	**P_D (single) W kg^{-1}**	**P_D (cell) W kg^{-1}**	**P_D (single) W kg^{-1}**	**P_D (cell) W kg^{-1}**
800.3	200.07	801.1	200.27	802.7	200.67	799.1	199.77	798.8	199.70
1601.2	400.3	1601.5	400.37	1607.7	401.92	1599.3	399.82	1593.6	398.40
2403.7	600.92	2405.6	601.4	2411.5	602.87	2402.1	600.52	2397.7	599.40
3201.7	800.42	3206.7	801.67	3228.7	807.17	3203	800.75	3193.9	798.47
3997	999.25	4022	1005.5	4038	1009.5	3996.9	999.22	3989.3	997.32

Table S8: *The specific capacitance values derived from CV and GCD for MCP ink based electrodes*

coated on carbon cloth.

Scan Rate ($mV\ s^{-1}$)	**Specific capacitance ($F\ g^{-1}$)**	**Current Density (Ag^{-1})**	**Specific capacitance ($F\ g^{-1}$)**
200	*199*	*1*	*573.5*
100	*310*	*2*	*531*
50	*423*	*3*	*490*
20	*530*	*4*	*465*
10	*585*	*5*	*400*
5	*669*		

Table S9: Extracted b, k_1, and k_2 values, along with the corresponding surface-controlled and diffusion-controlled charge-storage contributions of D-MXene, MC-20, and MCP electrodes, calculated using Dunn's method.

Electrode material	***b***	***k_1***	***k_2***	***Surface Controlled (%)***	***Diffusion controlled (%)***
D-MXene	*0.938*	*0.638*	*0.219*	*92.9*	*7.1*
MC-20	*0.986*	*0.522*	*0.037*	*98.4*	*1.6*
MCP	*0.869*	*0.603*	*0.453*	*85.6*	*14.4*

Table S10. *The calculated specific, C_{sp} and areal, C_{areal} capacitance values for the printed electrodes.*

Current (mA)	**C_{sp} ($F\ g^{-1}$)**	**C_{areal} ($mF\ cm^{-2}$)**
0.05	37.8	53
0.1	34.3	48
0.2	33.9	47.5
0.3	26.5	37
0.4	20.2	28

0.5	12	17

Table S11: *Fitted equivalent-circuit parameters of the D-MXene/MWCNT/PEDOT:PSS composite ink based printed MSC obtained from EIS analysis.*

Sl. No.	Element	Parameter	Value
1	R_S	Series resistance	63.52 Ω
2	Q	Constant Phase Element (CPE) magnitude	1.29×10^{-4}
3	n	CPE exponent	0.374
4	R_{ct}	Charge-transfer resistance	84.13 Ω
5	C_{dl}	Double-layer capacitance	6.11×10^{-4} F
6	R_1	Diffusion resistance	763.4 Ω
7	R_2	Interfacial/contact resistance	40.98 Ω
8	W	Warburg coefficient	3.93×10^{-4}
9	C	Low-frequency capacitance	4.92×10^{-3} F
10	R_3	Leakage resistance	2.238 kΩ
11	χ^2	Goodness of fit	9.346×10^{-5}

References

[1] S.M. Varghese, V. V. Mohan, S. Suresh, E. Bhoje Gowd, R.B. Rakhi, Synergistically modified Ti3C2Tx MXene conducting polymer nanocomposites as efficient electrode materials for supercapacitors, Journal of Alloys and Compounds 973 (2024) 695019.

https://doi.org/10.1016/j.jallcom.2023.172923.

[2] R.B. Rakhi, B. Ahmed, M.N. Hedhili, D.H. Anjum, H.N. Alshareef, Effect of Postetch Annealing Gas Composition on the Structural and Electrochemical Properties of Ti2CTx MXene Electrodes for Supercapacitor Applications, Chemistry of Materials 27 (2015) 5314–5323. https://doi.org/10.1021/acs.chemmater.5b01623.

[3] O. Mashtalir, M. Naguib, V.N. Mochalin, Y. Dall'Agnese, M. Heon, M.W. Barsoum, Y. Gogotsi, Intercalation and delamination of layered carbides and carbonitrides, Nature Communications 4 (2013) 1716. https://doi.org/10.1038/ncomms2664.

[4] W. Xu, Z. Xu, Y. Liang, L. Liu, W. Weng, Enhanced tensile and electrochemical performance of MXene/CNT hierarchical film, Nanotechnology 32 (2021). https://doi.org/10.1088/1361-6528/ac04cf.

[5] Q. Wang, H. Yuan, M. Zhang, N. Yang, S. Cong, H. Zhao, X. Wang, S. Xiong, K. Li, A. Zhou, A Highly Conductive and Supercapacitive MXene/N-CNT Electrode Material Derived from a MXene-Co-Melamine Precursor, ACS Applied Electronic Materials 5 (2023) 2506–2517. https://doi.org/10.1021/acsaelm.2c01768.

[6] X. Shi, F. Guo, K. Hou, G. Guan, L. Lu, Y. Zhang, J. Xu, Y. Shang, Highly Flexible All-Solid-State Supercapacitors Based on MXene/CNT Composites, Energy and Fuels 37 (2023) 9704–9712. https://doi.org/10.1021/acs.energyfuels.3c01420.

[7] Q. Liu, J. Yang, X. Luo, Y. Miao, Y. Zhang, W. Xu, L. Yang, Y. Liang, W. Weng, M. Zhu, Fabrication of a fibrous MnO2@MXene/CNT electrode for high-performance flexible supercapacitor, Ceramics International 46 (2020) 11874–11881. https://doi.org/https://doi.org/10.1016/j.ceramint.2020.01.222.

[8] Z. Wang, S. Qin, S. Seyedin, J. Zhang, J. Wang, A. Levitt, N. Li, C. Haines, R. Ovalle-Robles, W. Lei, Y. Gogotsi, R.H. Baughman, J.M. Razal, High-Performance Biscrolled

MXene/Carbon Nanotube Yarn Supercapacitors, Small 14 (2018) 1802225. https://doi.org/https://doi.org/10.1002/smll.201802225.

[9] H. Li, R. Chen, M. Ali, H. Lee, M.J. Ko, In Situ Grown MWCNTs/MXenes Nanocomposites on Carbon Cloth for High-Performance Flexible Supercapacitors, Advanced Functional Materials 30 (2020) 2002739. https://doi.org/https://doi.org/10.1002/adfm.202002739.

[10] R. Wang, S. Luo, C. Xiao, Z. Chen, H. Li, M. Asif, V. Chan, K. Liao, Y. Sun, MXene-carbon nanotubes layer-by-layer assembly based on-chip micro-supercapacitor with improved capacitive performance, Electrochimica Acta 386 (2021) 138420. https://doi.org/https://doi.org/10.1016/j.electacta.2021.138420.

[11] M. Tahir, L. He, W.A. Haider, W. Yang, X. Hong, Y. Guo, X. Pan, H. Tang, Y. Li, L. Mai, Co-Electrodeposited porous PEDOT-CNT microelectrodes for integrated micro-supercapacitors with high energy density, high rate capability, and long cycling life, Nanoscale 11 (2019) 7761–7770. https://doi.org/10.1039/c9nr00765b.

[12] A.S. Pillai, S.M. Varghese, R.B. Rakhi, S.K. Peethambharan, Synergistic effect of solvent addition and temperature treatment on conductivity enhancement of MWCNTs: PEDOT:PSS composite ink for electrodes in all printed solid-state micro-supercapacitors, Chemical Engineering Journal 495 (2024) 153495. https://doi.org/10.1016/j.cej.2024.153495.

[13] Q. Wang, Y. Fang, M. Cao, Constructing MXene-PANI@MWCNTs heterojunction with high specific capacitance towards flexible micro-supercapacitor, Nanotechnology 33 (2022) 295401. https://doi.org/10.1088/1361-6528/ac6432.